

# Generalized Disjunctive Programming Model for Optimization of Reverse Electrolysis Process

C. Tristán\*, M. Fallanza\*\*, I. Grossman\*\*, I. Ortiz\*, R. Ibáñez\*

\* *Department of Chemical and Biomolecular Engineering, University of Cantabria, Av. Los Castros 46, 39005 Santander, Spain (e-mail: {tristan, fallanzam, ortizi, ibanez}@unican.es).*

\*\* *Department of Chemical Engineering, Carnegie Mellon University, Pittsburgh, PA 15213, USA. (e-mail: grossmann@cmu.edu)*

---

**Abstract:** Reverse electrolysis (RED), an emerging electrochemical technology that uses ion-selective membranes to directly draw electricity out from salinity differences between two solutions, i.e., salinity gradient energy (SGE), could be a clean and steady renewable source to reach a sustainable water and energy supply portfolio. Although RED has made notable advances, full-scale RED progress demands more techno-economic and environmental assessments that consider full process design and operational decision space from module- to system-level. This work presents an optimization model formulated as a Generalized Disjunctive Programming (GDP) problem to define the cost-optimal RED process design for different deployment scenarios. We used a predictive model of the RED stack developed and validated in our research group to fully capture the behavior of the system. The problem addressed is to determine the RED plant's topology and the working conditions for a given design of each RED stack which renders the cost-optimal design for the defined problem and scenario. Our results reveal that, compared with simulation-based approaches, mathematical programming techniques are an efficient and systematic approach to provide decision-making support in early-stage applied research and to extract design and operation guidelines for full-scale RED implementation in real scenarios.

*Keywords:* renewable energy, blue energy, process synthesis, Pyomo, GDPopt, global optimization

---

## 1. INTRODUCTION

The progressive shift from conventional to low-emissions decentralized renewable power sources with little water needs will be decisive in reaching a sustainable water and energy supply portfolio. Reverse electrolysis (RED), an emerging electrochemical technology that uses ion-selective membranes to generate electricity out from the chemical energy released when two solutions of different salinities mix, i.e., salinity gradient energy (SGE), could be a clean and steady renewable source to power the water sector from the embedded energy of waste streams.

Past research has validated RED-based electricity from waste streams as desalination concentrates or treated wastewater effluents (Gómez-Coma *et al.*, 2020), but full-scale RED progress demands more techno-economic and environmental assessments that consider full process design and operational decision space from stack to the whole system. Our research group is working on a modelling tool to provide decision-making support for early-stage applied research and to extract design and operation guidelines for full-scale RED implementation in real scenarios.

We have developed and validated a predictive model of the RED stack to determine the most relevant working conditions and design parameters affecting RED performance (Ortiz-Imedio *et al.*, 2019; C. Tristán, M. Fallanza, *et al.*, 2020; Ortiz-Martínez *et al.*, 2020); This rigorous model allowed us to

assess the retrofit of medium-to-large-sized seawater reverse osmosis desalination plants across the globe with a RED-based energy recovery system through simulation (C. Tristán, Marcos Fallanza, *et al.*, 2020). If all SGE were harnessed, RED could meet ~40% of the desalination plant's energy demand almost in all locations but energy conversion losses and untapped SGE decline it to ~10%. These results denote there is a gap to bridge between the thermodynamic limit and the actual energy the RED system produces. Several variables affect the RED process, adding complexity to define optimal system designs by conventional trial and error evaluations. Hence, we propose an optimization model formulated as a Generalized Disjunctive Programming (GDP) problem to define the cost-optimal RED process design for different deployment scenarios.

## 2. OPTIMIZATION MODEL

### 2.1 Problem statement and superstructure definition

The formulation of the RED process synthesis problem can be stated as follows; Given the site-specific working conditions (i.e., the high-saline, HC, and low-saline, LC, feed streams' concentration, total flow rate, and temperature) and the stack design of all RED units (number of cell pairs, membrane's properties, spacers' thickness), the problem addressed is to determine the RED plant topology (i.e., number and hydraulic arrangement of the RED units) and the working conditions (i.e., the HC and LC concentration and flow rate, electric

current) of each RED stack in the RED plant that maximizes the net power output and net energy yield from the feed streams while minimizing cost of the RED process for the defined problem and scenario. We assumed the RED system operates under isothermal and isobaric conditions.

We have defined the superstructure of alternatives based on Pyosyn Graph (PSG) representation (Chen, Liu, *et al.*, 2021). The RED process PSG representation (Fig. 1) consists of the following representation elements:

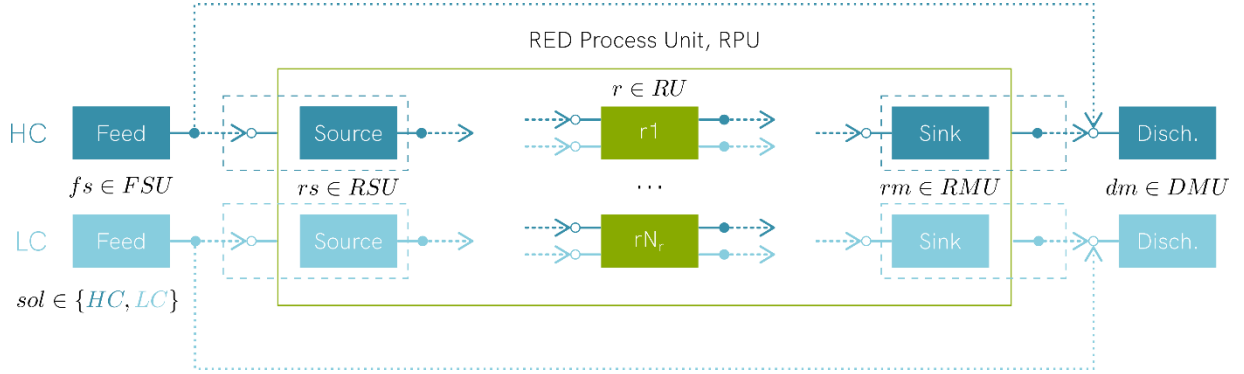


Figure 1 Superstructure representation of the RED process.

(a) The RED Process Unit (RPU), where discrete decisions on the selection of the RED units are made, which embeds: (i) the set of  $N_r$  candidate RED units  $r \in RU = \{r1, \dots, rNr\}$ ; the additional set of (ii) source  $rs \in RSU$  and (iii) sink  $rm \in RMU$  units for the high-salinity and low-salinity streams, i.e.,  $sol \in SOL = \{HC, LC\}$ , that govern the material in- and outflows for the overall flowsheet, respectively, and specifications on feed or effluent qualities of the RPU.

(b) The set of concentrate and diluate feed units,  $fs \in FSU$ , and discharge units,  $dm \in DMU$ .

(c) The inlet and outlet ports  $p \in P = P_{out} \cup P_{in}$ , —or mixers and splitters, respectively—, where flows of material at the unit interface with other process units may take place.

(d) The set of streams or feasible pairings of outlet ports to inlet ports,  $s \in S \subseteq P_{out} \times P_{in}$ , defined considering the following screening rules:

(i) The feed units,  $FSU$ , supply the concentrate and diluate feed streams to the RED Process Unit (RPU); While the discharge units  $DMU$  collect the exhausted high- and low-concentration RPU effluents, and the unused feed streams from the feed units  $FSU$ .

(ii) Within the RPU, the auxiliary source units,  $RMU$ , supply the concentrate and diluate streams coming from the feed units  $FSU$  to one or more of the active RED units. Once the active  $RU$  exploits SGE from the inlet streams, the exhausted effluents may be recycled back, sent to other active  $RU$  for reuse, or may be directed to the sink units,  $RMU$ . The RPU effluent from  $RMU$  is disposed of in the overall discharge unit  $DMU$ .

(iii) No flow between the  $RSU$  and  $RMU$  is allowed, only taking place between  $FSU$  and  $DMU$ .

(iv) Mixing between the concentrate and diluate streams only take place within the candidate RED units owing to the flow of ions from high-saline compartments to low-saline ones through ion-exchange membranes (IEMs).

Table 1 summarizes the indexes and sets of units, ports, and streams of the superstructure in Fig. 1.

## 2.2 Generalized Disjunctive Programming (GDP) model

We formulated the superstructure of alternatives as a Generalized Disjunctive Programming (GDP) problem coded in Python using the Pyomo algebraic modeling language (Hart *et al.*, 2017). The optimization model based on the superstructure in Fig. 1 is shown in the set of equations (1).

$$\begin{aligned}
 \min \text{obj} &= f(x) \\
 \text{s.t.} \quad &g(x) \leq 0 \\
 &\begin{bmatrix} Y_r \\ r_r(x) \leq 0 \end{bmatrix} \vee \begin{bmatrix} \neg Y_r \\ B^r x = 0 \end{bmatrix} \forall r \in RU \quad (1) \\
 &\Omega(Y_r) = \text{True} \\
 &x \in X \subseteq R^n \\
 &Y_r = \{\text{True}, \text{False}\} \forall r \in RU
 \end{aligned}$$

The objective function  $f(x)$  we want to optimize is the Levelized Cost of Energy (LCOE) of the RED process subject to inequality constraints (e.g., from process specifications) and equality constraints (e.g. from material, energy balances and thermodynamic relationships).

Variables  $x$  describe continuous decisions (e.g. molar concentrations, volumetric flows) of all feasible streams and the electric current of the candidate RED units.

Global constraints,  $g(x) \leq 0$ , are equalities and inequalities describing specifications and physical relationships that apply for all feasible configurations in the superstructure, e.g., flow and mass balances of the feed, source, sink, and discharge units' inlet and outlet ports, and the upper and lower bounds on streams' variables (concentration and flowrate).

Disjunctions, corresponding to logical-XOR relationships, such that at most one disjunct  $Y_r$  in each disjunction is True, describe the existence or absence of the RED units within the RED process unit. Boolean variables  $Y_r$  indicates whether a given RED unit exists or not. If a unit exists ( $Y_r = \text{True}$ ), the constraints  $r_r(x) \leq 0$  enforce the relevant mass and energy

balances, thermodynamics, kinetics, or other physical/chemical phenomena taking place within the RED unit. When the unit is absent, the negation ( $\neg Y_r$ ) sets to zero a subset of the continuous variables, and cost terms in the objective function through  $B^r x = 0$  constraints.

Mixing and splitting calculations when the port exists are included within the constraints  $r_r(x) \leq 0$ , and port absence in the linear constraints  $B^r x = 0$ . We adopt the no-flow approach for modeling an absent unit, enforcing that if a stream does not exist, no flow may take place between the corresponding outlet-inlet port pair.

Other types of logical relationships ( $\Omega(Y_r) = True$ ) are described using the following logical propositions:

(a) A logical constraint enforcing that at least one  $RU$  is active in the RPU section.

(b) Since all candidate RED units are equal, we added symmetry-breaking constraints (2) to avoid structural redundancy by eliminating symmetric solutions. Thus, easing computational effort.

$$Y_{r+1} \Rightarrow Y_r \quad \forall r \in RU \quad (2)$$

### 2.3 Flow and mass balance formulation

We formulated flow and mass balance equations considering total flows (volumetric flow rate,  $Q$  in  $m^3/h$ ) and species composition (molar concentration of sodium chloride,  $C$  in  $mol/m^3$ ), of the high- and low-saline streams.

The mixer' balances (3) apply to the inlet ports of the discharge units, the sink units, and the active RED units (i.e., when  $Y_r = True$ ). Mixing equations are nonlinear and nonconvex due to bilinear terms from the product of volumetric flowrate times molar concentration, that challenge finding a global optimum.

$$\begin{aligned} Q_{k,sol} C_{k,sol} &= \sum_{i \in S_i \subseteq S} Q_{i,sol} C_{i,sol} \\ Q_{k,sol} &= \sum_{i \in S_i \subseteq S} Q_{i,sol} \\ \forall sol \in SOL, k \in S_k \subseteq S \end{aligned} \quad (3)$$

The splitter' balances (4) apply to the outlet ports of the feed units, the source units, and the active RED units (i.e., when  $Y_r = True$ ). Splitting equations are linear and convex

$$\begin{aligned} C_{i,sol} &= C_{k,sol} \\ Q_{i,sol} &= \sum_{k \in S_k \subseteq S} Q_{k,sol} \\ \forall sol \in SOL, i \in S_i \subseteq S \end{aligned} \quad (4)$$

For the set of candidate RED units, the index  $k$  in splitting equations (4) is  $(r,ro)$  corresponding to the exhausted streams from RED's compartments leaving RED's outlet port; In the mixing equations (3), index  $i$  is  $(ri,r)$  defining the stream from the inlet port to the RED unit's compartments. The remainder index notations are summarized in Table 1.

**Table 1. Indexes and sets of units, ports, and streams of the RED process' superstructure.**

Unit	Streams			
	Port		$s \in S \subseteq P_{out} \times P_{in}$	
	In $P_{in}$	Out $P_{out}$	In $i \in S_i \subseteq S$	Out $k \in S_k \subseteq S$
Feed unit $fs \in FSU$	$fsi$	$fso$	$in,fsi^{**}$	$fso,rsi$ $fso,dmi$
Source unit $rs \in RSU$	$rsi$	$rso$	$fso,rsi$	$rso,ri$
RED unit* $r \in RU$	$ri$	$ro$	$rso,ri$ $ro',ri^{***}$	$ro,rmi$ $ro,ri^{***}$
Sink unit $rm \in RMU$	$rmi$	$rmo$	$ro,rmi$	$rmo,dmo$
Discharge unit $dm \in DMU$	$dmi$	$dmo$	$fso,dmi$ $rmo,dmi$	$dmo,out$

\*When the RED unit is active ( $Y_r = True$ ):  $k = (ri, r)$  in (3),  $i = (r, ro)$  in (4)

\*\*Known feed streams' composition and volume according to RED's implementation scenario.

\*\*\*Recycle or reuse

### 2.4 Bounds on variables

Using (5)–(7), we calculated the value, and upper (superscript U) and lower (superscript L) bounds of candidate RED units' flowrate. Each RED unit has upper limits on the inlet flowrate, according to the maximum linear cross-flow velocity (m/s),  $v_r^U$ , along the channel's length of the RED stack as manufacturer specifies. The lower bound  $v_r^L$  is at designer's disposal.  $v_{r,sol}$  is the average linear cross-flow velocity along RED units' channel length. The product  $N_{cp} \varepsilon_{sp,sol} b \delta_{sp}$  in (6) yields the cross-sectional area,  $A_r$  ( $m^2$ ), of all RED unit's compartments, where  $N_{cp}$  is the number of cell pairs,  $\varepsilon_{sp,sol}$  (-) the porosity,  $b$  (m) the width, and  $\delta_{sp,sol}$  (m) the thickness of the concentrate and diluate spacers, which are parameters of the RED stack model.

$$v_r^L \leq v_{r,sol} \leq v_r^U \quad \forall sol \in SOL, r \in RU \quad (5)$$

$$\begin{aligned} Q_{ri,r,sol} &= v_{r,sol} (N_{cp} \varepsilon_{sp,sol} b \delta_{sp,sol})_r \\ &= v_{r,sol} A_r \quad \forall sol \in SOL, r \in RU, ri \in P_{ri} \subseteq P_{in} \end{aligned} \quad (6)$$

$$\begin{aligned} Q_{ri,r,sol}^L &\leq Q_{ri,r,sol} \leq Q_{ri,r,sol}^U \\ \forall sol \in SOL, r \in RU, ri \in P_{ri} \subseteq P_{in} \end{aligned} \quad (7)$$

We used (8)–(10) to define the upper and lower limits on the concentrate and diluate streams' molar concentration (Table 2).

$$\begin{aligned} \phi_r^U &= \frac{Q_{ri,r,LC}^U}{Q_{ri,r,HC}^L + Q_{ri,r,LC}^U} \\ \phi_r^L &= \frac{Q_{i,LC}^L}{Q_{ri,r,HC}^U + Q_{ri,r,LC}^L} \\ \forall r \in RU, r \in RU, ri \in P_{ri} \subseteq P_{in} \end{aligned} \quad (8)$$

where  $\phi(-)$  is the ratio of diluate solution's flowrate to total flowrate that is fed to the RED unit.

$$\begin{aligned} C_{M,r}^U &= \phi_r^L \max_{i \in S_{fsi} \subseteq S_i} (C_{i,LC}) + (1 - \phi_r^L) \max_{i \in S_{fsi} \subseteq S_i} (C_{i,HC}) \\ C_{M,r}^L &= \phi_r^U \min_{i \in S_{fsi} \subseteq S_i} (C_{i,LC}) + (1 - \phi_r^U) \min_{i \in S_{fsi} \subseteq S_i} (C_{i,HC}) \\ &\quad \forall r \in RU \end{aligned} \quad (9)$$

$C_{M,r}$  (mol/m<sup>3</sup>) is the concentration of the mixed solution reaching equilibrium.

$$C_{sol}^L \leq C_{s,sol} \leq C_{sol}^U \quad \forall sol \in SOL, s \in S \quad (10)$$

The upper bound on concentrate streams' concentration could be as high as the maximum concentration of the feed streams, *in* (if there are multiple feed alternatives), while for the diluate streams, the molar concentration could be as high as the concentration reached after the complete mixing of the concentrate and diluate stream (if reached thermodynamic equilibrium). The opposite goes for the lower bound on the concentration of the concentrate and diluate streams.

**Table 2. Upper and lower bounds on concentration of superstructure's streams**

Bounds	$sol = HC$	$sol = LC$
$C_{sol}^U$	$\max_{i \in S_{fsi} \subseteq S_i} (C_{i,HC})$	$C_{M,r}^U$
$C_{sol}^L$	$C_{M,r}^L$	$\min_{i \in S_{fsi} \subseteq S_i} (C_{i,LC})$

### 2.5 RED stack model formulation

We used a simplified version of the RED stack's rigorous model from our research group (C. Tristán, M. Fallanza, *et al.*, 2020), to find a middle-ground between model fidelity and tractability.

The semi-rigorous model is a system of differential and algebraic equations defining RED's behavior from cell pair to module-scale. A cell pair is a repeating unit stacked in series to form the RED pile, assembled alternating a cation- and an anion-exchange membrane (CEM and AEM, respectively) with two adjacent spacer-filled compartments where the concentrate and the diluate water streams flow.

The cell pair model describes the main transport mechanisms across membranes, mass balances, distributed pressure drop, and the electric variables, i.e., the potential difference and internal resistance, within a cell pair. The differential mass balance equations in the diluate and the concentrate solution, linked by mass transfer equations, define the bulk ionic concentration and flow rate distributions along the channels. The mass transport equations provide the mass flux of sodium chloride across membranes from the HC side to the LC one.

At RED stack's scale, the model computes the overall values (electric potential, electric current, internal resistance, pressure drop) of the whole set of series cell pairs averaging each distributed variable in the flow direction (taking the integral over the length domain,  $x$ ). The model also computes the gross and net power output (deducting the pumps' power consumption from the gross power output) to define

performance metrics as power density, energy yield, and specific energy of the RED stack and to compute the net power output of the RED system.

With the following simplifying assumptions:

- The feed streams are pure sodium chloride, ideal (i.e. activity coefficients equal to 1) aqueous solutions, thus neglecting the non-idealities of aqueous solution and existence of other species that would undermine RED performance.
- There is no non-ohmic contribution in the internal losses ascribed to concentration polarization phenomena in the concentrate and diluate membrane-solution interfaces, and concentration gradient decline along the main flow direction. We only considered ohmic contribution due to solutions' ionic conductivity and membranes' ionic resistance.
- Membranes' permselectivity and ionic resistance are constant regardless of solutions' concentration and temperature.
- There is no water transport due to osmosis from the low-saline side to the high-saline one across membranes.
- Salt diffusivities in the membrane phase are constant whatever concentration and temperature.
- All cell pairs behave equally, as we assumed no fluid leakage or ionic shortcut currents in the RED stack's manifolds.
- Co-current flow of the high- and low-concentration streams.

The reader is referred to work (C. Tristán, M. Fallanza, *et al.*, 2020) for more details on the RED stack model.

As optimization solvers are unable to handle integrals or differential equations directly, we applied the backward finite difference method and the trapezoid rule to reformulate first-order ordinary differential equations, and integrals into algebraic equations, respectively.

When the RED unit is active ( $Y_r = \text{True}$ ), the boundary conditions (11) link the inlet port  $ri$  with the RED unit's inlet compartments (i.e., when  $x = 0$ ), and (12) the outlet from the set of cell pairs (i.e., when  $x = L$ ) with the outlet port  $ro$  of the RED unit.

$$\begin{aligned} C_{ri,r,sol} &= C_{0,r,sol} \\ Q_{ri,r,sol} &= N_{cp} Q_{0,r,sol} \\ \forall sol \in SOL, r \in RU, ri \in P_{ri} \subseteq P_{in} \end{aligned} \quad (11)$$

$$\begin{aligned} C_{r,ro,sol} &= C_{L,r,sol} \\ Q_{r,ro,sol} &= N_{cp} Q_{L,r,sol} \\ \forall sol \in SOL, r \in RU, ro \in P_{ro} \subseteq P_{out} \end{aligned} \quad (12)$$

When the RED unit is absent ( $\neg Y_r$ ) (13) applies, and the net power output and cost terms in the objective function are set to zero.

$$\begin{aligned}
C_{sr,sol} &= C_{sol}^L, \forall sr \in S_{ri} \cup S_{ro} \\
\sum_{i \in S_{ri} \cup S_{ro}} Q_{i,sol} &= 0, \\
Q_{rso,ri,sol} &= 0 \forall rso \in P_{rso}, ri \in P_{ri} \\
&\forall sol \in SOL
\end{aligned} \tag{13}$$

### 2.6 Objective function: Levelized Cost of Energy (LCOE)

The objective of the GDP problem is to minimize the LCOE of the RED process. The LCOE (USD<sub>2019</sub>/kWh), a common metric to benchmark different renewable power technologies, estimates the average cost per unit of energy generated across the lifetime of a power plant. The LCOE considers operating (OPEX in USD<sub>2019</sub>/year), and capital costs (CAPEX in USD<sub>2019</sub>) annualised over the expected lifetime of the plant, LT in years, using the capital recovery factor (CRF) given in (15) with an interest rate  $r$ , that altogether define the total annual cost of the RED system.

Assuming the energy provided annually is constant during the lifetime of the project, the LCOE reduces to (14). The annual energy yield (kWh/year) of the RED plant working at full capacity, i.e., 8760 full load hours per year, is corrected with a load factor, LF, of 90% (i.e., RED works 8000 hours each year). The summation of the net power output over the candidate RED units yields the nominal capacity of the RED system (16).

$$LCOE = \frac{CRF CAPEX + OPEX}{TNP 8760 LF} \tag{14}$$

$$CRF = \frac{r}{1 - (1 + r)^{-LT}} \tag{15}$$

$$TNP = \sum_{r \in RU} NP_r \tag{16}$$

To estimate the capital investment, we determine the cost of RED units, pumps, and civil and electrical infrastructure cost.

$$CAPEX = CC_{stack} + CC_{pump} + CC_{civil} \tag{17}$$

The annual operating cost comprises the electricity cost from pumps' consumption, the replacement cost of the RED membranes, and maintenance and labor costs (as 20% of CAPEX).

$$OPEX = OC_{pump} + OC_{IEMsrep} + 0.2 CAPEX \tag{18}$$

Wherever needed, all currencies were converted to USD<sub>2019</sub> according to historical average exchange rate of the corresponding publication year.

### 2.7 Solution strategy

For the solution of the GDP problem, we used the logic-based solver GDPopt built on Pyomo.GDP, an open-source ecosystem for GDP modeling and development, built on top of the Pyomo algebraic modeling language (Chen, Johnson, *et al.*, 2021).

We apply the Global Logic-based Outer Approximation (GLOA) algorithm (Lee and Grossmann, 2001; Chen *et al.*, 2018) to solve the GDP problem. This strategy decomposes the GDP into reduced NLP subproblems and Master MILP problems, to avoid “zero-flow” numerical issues arising in nonlinear design problems when units or streams disappear.

## 3. CASE STUDY: ENERGY RECOVERY FROM DESALINATION CONCENTRATE

We consider as a case study the retrofit of several medium-to-large capacity seawater reverse osmosis (SWRO) desalination plants distributed worldwide with a RED-based energy recovery system; The RED plant retrieves electric energy from desalination's concentrate effluent reversibly mixed with different available low-salinity sources (e.g., WWTP effluent, seawater, river water). Data on concentration, temperature, and volumetric flow rate of the high- and low-saline feed streams are taken from (C. Tristán, Marcos Fallanza, *et al.*, 2020).

To compare the performance of the fixed series-parallel arrangement of the RED units, set in our previous assessment (C. Tristán, Marcos Fallanza, *et al.*, 2020), with the hydraulic topology the optimization model gives, we restricted our study to one parallel branch setting the flow rate and concentration of the inlet streams to each parallel branch equal to the optimal working conditions of the 1<sup>st</sup> RED unit in the series for two hydraulic arrangements:

(a) Series layout, from our former study, imposing that the outlet stream of the RED unit is fed to the inlet port of the following series unit, so recycling or alternative reuse options of the outlet streams are not allowed.

(b) GDP layout, leaving the interconnection between the superstructure units free as a discrete decision.

The upper limit of parallel branches was set considering the RED system treats desalination's concentrate effluent in full, assuming no shortage of low-saline feed stream. Then, the net power output of the RED system scales with the number of parallel branches.

The assessment refers to a commercial RED unit with an assumed number of cell pairs representative of industrial-scale stacks. Data on RED stack's parameters and process specifications can be found on (C. Tristán, Marcos Fallanza, *et al.*, 2020).

## 4. RESULTS AND DISCUSSION

The optimization model provides an optimized RED's flowsheet design in all scenarios improving the cost-competitiveness of the system compared with the series-parallel arrangement. As an illustrative example, we show the optimization results for the RED-retrofit of Barcelona-Llobregat SWRO desalination plant (Sanz and Miguel, 2013; C. Tristán, Marcos Fallanza, *et al.*, 2020).



**Table 3. Optimization results of a parallel branch in the RED system for the fixed and decision hydraulic arrangement of the RED units.**

	Layout	
	Series (fixed)	GDP (decision)
# RED units	5	6
TNP (kW)	3.0	3.4
LCOE (USD <sub>2019</sub> /MWh)	174	158
CAPEX (kUSD <sub>2019</sub> )	23.64	24.36
OPEX (kUSD <sub>2019</sub> /year)	1.78	1.86

Case study:  $N_r = 15$ ; RED stack working conditions (HC/LC): 1.23/0.04 mol/L, 7.24/9.87 m<sup>3</sup>/h, 19 °C;

The GDP optimization model renders a flowsheet design that reduces the LCOE and increases the net power output of the RED system by 9% and 14%, respectively, which in turn could save around 20% of the desalination plant's specific energy consumption sourced by the local grid mix.

## 5. CONCLUSIONS

In this work, we propose a GDP optimization model to systematically synthesize and optimize the RED process for electricity production from salinity gradient energy. The goal is to define the hydraulic topology, that is, the number and hydraulic layout of the set of candidate RED units, and the working conditions of each RED stack that minimize the LCOE, used as a metric to measure RED process economic competitiveness in a given application scenario. Simulation-based approaches on conceptual design fail to handle complex systems with high degrees of freedom which may lead to suboptimal solutions; Hence, to illustrate how mathematical programming techniques could enhance RED process conceptual design over conventional trial-and-error procedures, we evaluated RED energy recovery from desalination's concentrate effluent around the world for two hydraulic configurations: (i) a fixed series-parallel arrangement of the RED units with no recycle or additional reuse alternatives of the exhausted water streams after SGE retrieval and (ii) freeing the layout to accommodate all feasible reuse and recycle alternatives. Compared with the simulation-based approach from our previous study, the optimization model provides a RED's flowsheet design that improves the cost-competitiveness of the system in all scenarios. Our results reveal mathematical programming techniques as an efficient and systematic decision-making approach over simulation alone to advance RED's Technology Readiness Level. The process synthesis model could be a valuable tool to assist RED field demonstration and deployment stages in real environments.

Future work will test different solution strategies and problem formulations to improve the computational effort and robustness of the model, extend the superstructure of alternatives with more discrete and continuous decision variables, related to RED stack design (e.g. the number of cell pairs, membranes' and spacer's design) and the RED system (e.g., adding auxiliary equipment as DC-AC inverters, or

processes as pre-treatment of feed's solutions), consider environmental concerns through multi-objective optimization.

## ACKNOWLEDGEMENTS

Project LIFE19 ENV/ES/000143 funded by the LIFE Programme of the European Union. Grant PDC2021-120786-I00 funded by MCIN/AEI/10.13039/501100011033 and by the "European Union NextGenerationEU/PRTR". Grant PRE2018-086454 funded by MCIN/AEI/10.13039/501100011033 and by "ESF Investing in your future".

## REFERENCES

- Chen, Q. *et al.* (2018) "Pyomo.GDP: Disjunctive Models in Python," in *Computer Aided Chemical Engineering*. Elsevier B.V., pp. 889–894.
- Chen, Q., Johnson, E. S., *et al.* (2021) "Pyomo.GDP: an ecosystem for logic based modeling and optimization development," *Optimization and Engineering*, pp. 1–36..
- Chen, Q., Liu, Y., *et al.* (2021) "Pyosyn: a new framework for conceptual design modeling and optimization," *Computers & Chemical Engineering*, p. 107414.
- Gómez-Coma, L. *et al.* (2020) "Blue energy for sustainable water reclamation in WWTPs," *Journal of Water Process Engineering*, 33, p. 101020.
- Hart, W. E. *et al.* (2017) *Pyomo — Optimization Modeling in Python*. Second Edi. Cham: Springer International Publishing (Springer Optimization and Its Applications).
- Lee, S. and Grossmann, I. E. (2001) "A global optimization algorithm for nonconvex generalized disjunctive programming and applications to process systems," *Computers and Chemical Engineering*, 25(11–12), pp. 1675–1697.
- Ortiz-Imedio, R. *et al.* (2019) "Comparative performance of Salinity Gradient Power-Reverse Electrodialysis under different operating conditions," *Desalination*, 457, pp. 8–21.
- Ortiz-Martínez, V. M. *et al.* (2020) "A comprehensive study on the effects of operation variables on reverse electrodialysis performance," *Desalination*, 482, p. 114389. doi: 10.1016/J.DESAL.2020.114389.
- Sanz, M. A. and Miguel, C. (2013) "The role of SWRO Barcelona-Llobregat Plant in the water supply system of Barcelona Area," *Desalination and Water Treatment*, 51(1–3), pp. 111–123.
- Tristán, C., Fallanza, M., *et al.* (2020) "Recovery of salinity gradient energy in desalination plants by reverse electrodialysis," *Desalination*, 496, p. 114699.
- Tristán, C., Fallanza, Marcos, *et al.* (2020) "Reverse electrodialysis: Potential reduction in energy and emissions of desalination," *Applied Sciences (Switzerland)*, 10(20), pp. 1–21.